Gas-Liquid Two-Phase Flow in Symmetrically Dividing Horizontal Tubes

L. Lightstone, S. I. Osamusali, and Jen-Shih Chang
Dept. of Engineering Physics, McMaster University, Hamilton, Ontario, Canada L8S 4M1

The time-averaged void fraction, pressure drop and flow regime transition behavior of horizontal air-water two-phase flows is studied experimentally and numerically for 2-cm-inner-diameter tubes with various flow dividing junctions at its end. The time-average void and pressure drop behavior along the channel is simulated using a two fluid separated flow model. The results show that two-phase behavior (flow regime, void fraction, and pressure drop) is affected strongly by the presence of a flow division in the system. These effects extend far upstream of the junction for low-momentum flows and far downstream for high-momentum flows. Both numerical and experimental results show that there occurs a large increase in void just downstream of the junction owing to the halving of the fluid volume flow rates and the liquid deceleration.

Introduction

Two-phase flow is becoming increasingly important in many areas of engineering design such as gas distribution lines, heat exchanger analysis, and power plant heat transport systems. Although complete analytical formulations of the equations describing these flows have been developed, their complexity makes them exceptionally cumbersome. As a result, many researchers have spent their time producing "constitutive laws" describing two-phase systems. However, it still remains for many of the above-mentioned constitutive laws to be tested in the more complex situations such as the accelerating conditions that arise in a flow dividing system. This work examines a particular two-phase system and attempts a numerical and experimental analysis to successfully describe the phenomena observed in the flow dividing and nondividing configurations.

Single-phase flows in dividing junctions have been studied very early on in the engineering literature (McNown, 1954; Modi et al., 1981). The standard approach is to consider the pressure drop in terms of a Bernoulli-type equation

$$P_1 + \rho\frac{u_1^2}{2} = P_2 + \rho\frac{u_2^2}{2} + \Omega\rho\frac{u_1^2}{2}$$

where P and u are the fluid pressure and speed, and 1 and 2 correspond to upstream and downstream of the "flow perturbation." Here, the irreversible work done on the fluid is represented by a loss coefficient Ω, which multiplies a kinetic energy term. These loss coefficients have been well tabulated.

The single-phase problem of inviscid irrotational junction flow was considered by Modi et al. (1981), and analytical solutions were arrived at using the method of conformal mapping. Recently computer studies of three-dimensional single-phase turbulent and laminar flows in flow dividing tee junctions have been conducted by Pollard and Spalding (1978, 1980, 1981).

When considering a two-phase flow in a dividing junction, two additional complications must be accounted for that do not arise in the single-phase case. They are:

- Change in void fraction near junction site
- Change in flow regime structure near junction site.

Very few studies have been done on horizontal two-phase dividing flow. These studies (Tsuyama and Taga, 1959; Fouda and Rhodes, 1972, 1974; Henry, 1981; Honan and Lahey, 1981; Azzopardi and Whalley, 1982; McCreery, 1983; Seeger et al., 1986; Reimann and Seeger, 1986; Ballyk et al., 1988) have not considered any effect of flow regime change nor have they examined void fraction behavior but have confined themselves to the study of pressure drop and flow quality division.

These regimes result from the particular manner in which the two phases are distributed in the pipe. Though authors

L. Lightstone is presently at the Atlantis Scientific, Ottawa, Ontario, Canada, K2C 0P9, and S. I. Osamusali at the Ontario Hydro, Toronto, Ontario, Canada M5G 1X6.

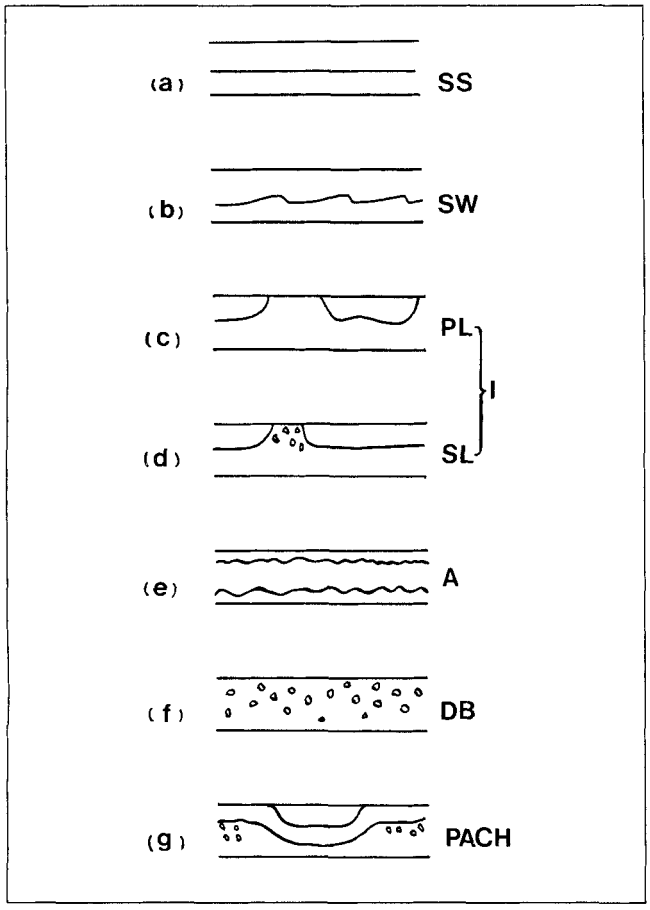

Figure 1. Horizontal two-phase flow.

a. Stratified smooth; b. stratified wavy; c. plug; d. slug; e. annular; f. dispersed bubble; g. periodic annular churn.

define each flow regime somewhat differently, most agree that there are six basic structures. Examples of these flows are shown in Figure 1. In this study the flow regime analysis will be based on the definitions below.

Stratified smooth (SS) flow occurs when the liquid is at the bottom of the pipe and the gas flows along the top. The surface of the liquid is smooth. Stratified wavy (SW) flow is similar to stratified smooth; however, the gas-liquid interface is wavy. Both elongated bubble [designated as plug (PL) flow] and slug (SL) flow are what Taitel and Dukler (1976) call intermittent (I) flow and are characterized by the liquid bridging the gap between the gas-liquid interface and the top of the pipe. The difference between slug and plug flow depends on the degree of agitation of the bridge. This work follows the definition of Taitel and Dukler (1976). Plug flow is considered to be the limiting case of slug flow where no entrained bubbles exist in the liquid slug.

Annular flow (A) occurs when the walls are wetted by a thin film of liquid, while the gas at high velocity flows through the center of the pipe. Liquid droplets are usually entrained in this gas. When the upper walls are wetted periodically by large aerated waves, it is neither slug flow requiring a complete fluid bridge nor annular flow requiring a stable film. Taitel and Dukler (1976) designated this flow pattern as wavy annular flow. This regime, however, was not recognized by Mandhane et al. (1974) and was considered to be slug flow.

In the dispersed bubble (DB) or bubbly regime, small gas bubbles are distributed throughout the liquid phase which otherwise completely fills the pipe. The transition to this regime is characterized by the gas bubbles losing contact with the top of the tube. At first, the bubbles are near the upper portion of the pipe, but at higher liquid flow rates become uniformly distributed throughout the system.

Periodic annular (PA) flow occurs when the annular liquid film tends to wrap itself around the inner wall at junctions as experimentally observed as shown in Figure 1.

Momentum Analysis of Two-Phase Dividing Flow

A flow dividing junction may be viewed as a sudden expansion in a one-dimensional sense because of the increase in the area available for the flow. In the single-phase analysis, an expression for the loss coefficient of a sudden expansion was derived by considering a momentum balance on a control volume surrounding the junction and assuming that the pressure before and after the expansion was derived by considering a momentum balance on a control volume surrounding the junction and assuming that the pressure before and after the expansion acted on the area downstream of the junction. This was experimentally shown to yield the correct value for the loss coefficient (Schutt, 1929):

$$\Omega = \left(1 - \frac{A_1}{A_2}\right)^2.$$

The two-phase analogy of the above was postulated by Lottes (1961) as:

$$A_1P_1 + \rho_g Q_{g_1} u_{g_1} + \rho_\ell Q_{\ell_1} U_{\ell_1} = A_2P_2 + \rho_g Q_{g_2} u_{g_2} + \rho_\ell Q_{\ell_2} U_{\ell_2}.$$

This equation was experimentally tested by Lottes (1961) and shown to provide a reasonably good method for pressure drop evaluation.

To construct the equations describing the time-averaged two-phase dividing flow, the two fluids are assumed to be stratified. In a straight section of flow tubes before and after the junction, it is assumed that there is little change in the void fraction. In these regions, a simple two-fluid separated-flow model is applied. At the junction it is assumed that there is a significant change in void fraction. The momentum equations are constructed by considering control volumes surrounding each fluid at the junction. The irreversible losses that occur at the junction location are considered in two parts:

a. Losses due to a sudden expansion
b. Losses due to the turning of the fluid.

Loss (a) is incorporated into the equations through Lottes's formulation. The modeling of loss (b) follows the single-phase analysis of incorporating a loss factor (Ω) multiplying a kinetic energy term. It is assumed that $\Omega = \Omega(\theta)$ where θ is the junction angle and that $\Omega = 0$ for $\theta = 0$. In other words, if the system is a true sudden expansion there should be no "fluid turning" losses. In addition to the above loss terms, a special momentum exchange term is included at the junction to account for enhanced fluid-fluid interactions there. The flow regime structure and fluid friction terms are taken into account through the use

of the constitutive laws which are developed for the straight pipe system.

Momentum model for two-phase dividing flow

This section is concerned with the modeling of the pressure drop and void fraction throughout the flow dividing system. The flows are considered incompressible and time-averaged, and thus may be described as both stratified and time-independent. In a straight section of flow tubes before and after the junction, it is assumed that there is little change in void fraction along the tube. The flows in these regions may therefore be described by Newton's law for each phase j.

$$\rho_j u_j \frac{du_j}{dz} = -\left(\frac{dP}{dz}\right)_j + F_j \tag{1}$$

Here a one-dimensional analysis is considered and the steady-state assumption has been applied.

For the liquid, body forces consist of the wall and interfacial friction, and gravity forces. In the gas phase, gravity forces are neglected, and only wall and interfacial frictions are accounted for. These friction terms contain the flow regime information. It is also assumed, as with the majority of the analysis done in this text, that the pressure drops in each phase are equal.

Writing the equations of motion for each phase in full:

$$\rho_g u_g \frac{du_g}{dz} = -\frac{dP}{dz} - \frac{\tau_g S_g}{A_g} - \frac{\tau_i S_i}{A_g} \tag{2}$$

$$\rho_\ell u_\ell \frac{du_\ell}{dz} = -\frac{dP}{dz} - \frac{\tau_\ell S_\ell}{A_\ell} - \frac{\tau_i S_i}{A_\ell} - \rho_\ell g \frac{dh_\ell}{dz} \tag{3}$$

Subtracting Eq. 2 from Eq. 3 yields the following:

$$\rho_\ell u_\ell \frac{du_\ell}{dz} - \rho_g u_g \frac{du_g}{dz} = \Psi - \rho_\ell g \frac{dh_\ell}{dz} \tag{4}$$

where

$$\Psi = -\frac{\tau_\ell S_\ell}{A_\ell} + \frac{\tau_g S_g}{A_g} + \tau_i S_i \left(\frac{1}{A_g} + \frac{1}{A_\ell}\right) \tag{5}$$

The flow dividing junction is considered in a one-dimensional sense. To develop the momentum equations at the junction site, consider two control volumes around each fluid as shown by the dotted lines in Figure 2. The junction is assumed to expand in a direction into the page to twice the area of the upstream pipe.

Conservation of linear-momentum over a control volume CV bounded by a control surface CS may be written as

$$\Sigma \text{ Forces} = \frac{d(mu)}{dt} = \frac{\partial}{\partial t}\int_{cv} \rho u dV + \int_{cs} \rho u (u \cdot dA) \tag{6}$$

For our analysis, applying the one-dimensional steady-state assumptions, Eq. 6 may be rewritten for a given phase j

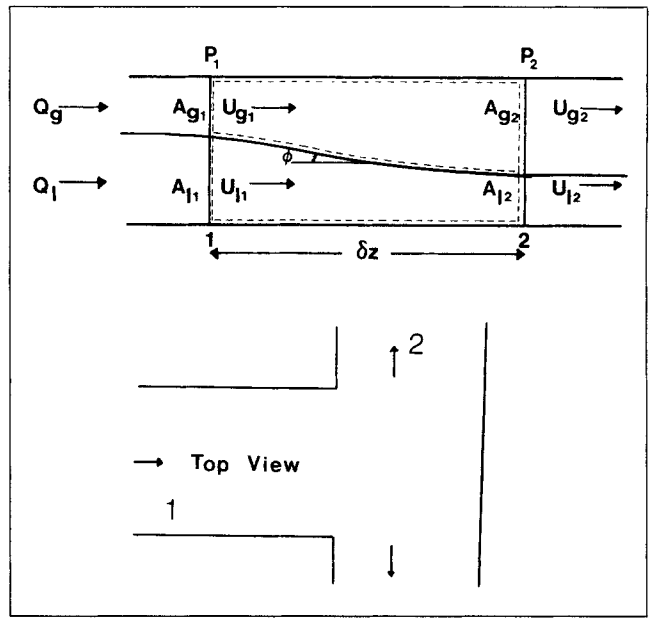

Figure 2. Control volumes at junction site.

$$A_{1_j} P_{1_j} - A_{2_j} P_{2_j} + g\left(h_{1_j} A_{1_j} - h_{2_j} \frac{A_{2_j}}{2}\right) - f_j \delta z = \rho_j Q_j (u_{2_j} - u_{1_j}) \tag{7}$$

where f represents the friction terms

$$f = \tau S\Big|_w \pm \tau S\Big|_i \cos\Phi \tag{8}$$

with

$$\tau S = \frac{1}{\delta z}\int_{cs} \tau(z) S(z) dz \simeq \tau S\Big|_2 \tag{9}$$

w corresponds to wall friction, i to interfacial friction, and $\pm$ depends on the phase under consideration. Furthermore, it is assumed that Φ is small so that $\cos\Phi = 1.0$. Note also that the gravitation term at location 2 is divided by 2. This assumes that the "hydrostatic" forces upstream of the junction act only on the downstream projected area $(A_1/2)$ and that the remainder of the "hydrostatic" force exerted downstream of the junction is "supported" by the wall of the sudden expansion.

In this analysis, it is assumed that the irreversible losses (with the exception of friction) occur solely at the junction site. These losses are considered in two parts:

a. Sudden expansion losses
b. Turning losses.

In addition to the above, there is also the possibility of enhanced momentum exchange at the junction because of the fluid-fluid interaction there. This will be accounted for by considering a turning-momentum-exchange term.

Neglecting gravitational effects on the gas phase and accounting for the sudden expansion loss by assuming that P_1 acts on A_2, the momentum equations at the junction become

$$A_{2_g}P_1 - A_{2_g}P_2 - (\tau_{g_2}S_{g_2} + \tau_{i_2}S_{i_2})\delta z = \rho_g Q_g(u_{g_2} - u_{g_1}) + \Omega_g(\theta) + \Omega(\theta) \quad (10)$$

$$A_{2_\ell}P_1 - A_{2_\ell}P_2 - (\tau_{\ell_2}S_{\ell_2} + \tau_{i_2}S_{i_2})\delta z + \rho_\ell g\left(h_1 A_{\ell_1} - h_2\frac{A_{\ell_2}}{2}\right) = P_\ell Q_\ell(u_{\ell_2} - u_{\ell_1}) + \Omega_\ell(\theta) - \Omega'(\theta) \quad (11)$$

where $\Omega_\ell(\theta)$ and $\Omega_g(\theta)$ represent the losses due to the turning of the indicated fluid and $\Omega'(\theta)$ represents the turning-momentum exchange between the fluids.

If the friction, gravity and "turning" terms in Eqs. 10 and 11 are neglected, addition of these two equations will yield the expression developed by Lottes (1961) indicating that the losses due to sudden expansion have been properly accounted for.

To choose the form of Ω's, we again extrapolate from single-phase procedures:

$$\Omega_j(\theta) = \Omega_0 \rho_j A_j \frac{u_{j_1}^2}{2}\sin^a\theta \quad (12)$$

The constant Ω_0 is assumed to be the same for single-phase flow and is given a value of 1.55. The angular dependence has been included to fit the extreme conditions. The exponent a will be experimentally determined.

The remaining term in the junction equations, $\Omega'(\theta)$, represents the momentum exchange between the two fluids at the junction. The expression for this exchange term is chosen to be similar in structure to that of Eq. 12. However, the properties of both fluids should be accounted for and so the following is used:

$$\Omega'(\theta) = \Omega_0' \rho_{2\phi} A \frac{(u_g - u_\ell)^2}{2}\sin^a\theta \quad (13)$$

where

$$\rho_{2\phi} = (A_g\rho_g + A_\ell\rho_\ell)\frac{1}{A} \quad (14)$$

In the above equation, Ω_0' is an experimentally determined constant. With the evaluation of the Blasius parameters from the linear two-phase configuration, the flow dividing system is described with two constants Ω_0' and a.

The initial conditions, "far away" from the junction, are determined by assuming that the fluids do not "see" the junction. In other words, the acceleration and gravity terms are equal to zero. Thus, the initial speeds may be determined for given flow rates by setting Ψ (Eq. 5) equal to zero.

With the inclusion of the equations of continuity

$$u_j A_j = Q_j \quad (15)$$

and experimental determination of the Blasius constants used in evaluation of the friction terms, the above set of equations is closed. The momentum equations listed above are evaluated using the finite difference iterative scheme.

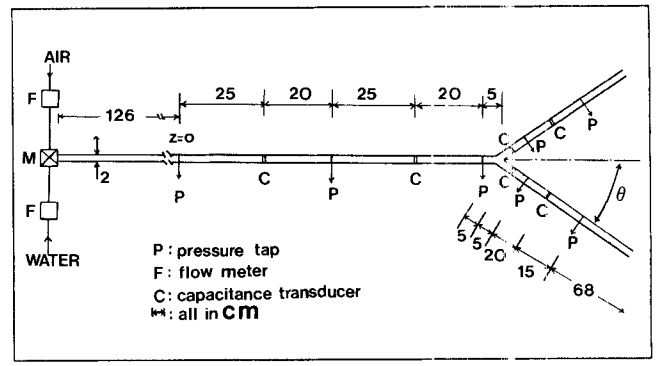

Figure 3. Experimental apparatus.

Fluids enter the mixing section (M) through a filter (F), a pressure regulator (R), valves (V), and flowmeters (FM). Differential pressure readings are taken at pressure taps (P). Void fraction readings are taken at capacitance transducer locations (C).

Experimental Apparatus

The top view of the experimental apparatus for the two-phase experiments is shown in Figure 3. Water and compressed air are taken from the laboratory supply at approximate room temperature. The air is passed through a filter and a pressure regulator. Each fluid is passed through its own series of valves and flowmeters that are used to monitor the flow. The two fluids then enter a horizontal pipe through a glass-bead mixing section, which is used to enhance the onset of fully developed two-phase flow.

The pipe itself is constructed of 2-cm-diameter segmented glass pipes connected by brass joiners, which also supply the pressure taps for the system. The Wyes are one-piece smooth-edged glass sections of the same inner diameter as the main pipe. Different Wyes are attached to the main pipe by the above-mentioned brass joiners. The two ends of the flow dividing the section are open to the atmosphere. A weighing tank is located at one of the Wye section ends for the flow quality measurement while the other branch is connected directly to a central drain.

Void fraction was determined by four ring-type capacitance transducers (Chang et al., 1984) positioned on the outer surface of the tube as shown. The ring electrodes are used in conjunction with a Booton 72-B capacitance meter. The void measurement system is calibrated *in situ* using stratified water conditions (since the capacitance ring configuration is almost independent of flow regime (Chang et al., 1984) and the ultrasonic liquid-level measurement system (Chang et al., 1982; Matikainen et al., 1986).

Differential pressure drop measurements were obtained using Validyne DP15 and DP105 pressure transducers, for large and small pressure drops, respectively, along with a Validyne CD-123 pressure demodulator. Differential pressure measurements are taken with respect to the pressure tap farthest from upstream of the junction. The pressure sampling position is controlled through multiple-input switching valves.

The void fraction and pressure waveforms were sampled "simultaneously" at a rate of 30 samples/second by a Nova III minicomputer. Time-averaged values of these quantities were obtained through multiple averaging of waveforms of 10-s duration. The important statistical parameters for these av-

erages, standard deviation, and maximum deviation are obtained for each measurement. A sample waveform along with time-averaged data for each measurement was recorded on magnetic tape for later access. The pressure and void fraction waveforms are also used for characterization of flow regimes (Lightstone et al., 1983).

In this study, four different test sections were used: a symmetric tee, and a 60°, 45° and 30° symmetric Wye all positioned in the horizontal plane. Flow regime observations were made at four different locations: 1. 37 pipe diameters upstream of the junction, L_1; 2. 14 pipe diameters upstream of the junction, L_2; 3. two pipe diameters downstream of the junction, L_3; and 4. 25 pipe diameters downstream of the junction, L_4. Symmetry of flow regime on both sides of the junction was observed for each flow condition. Observations were made at locations sufficiently far from the inlet and the outlet of the tube to prevent pipe entrance and exit effects from interfering with the results. Each flow regime map was constructed from an experimental array of 110 points consisting of liquid and gas superficial velocities ranging from 1 to 18 cm/s and 10 to 265 cm/s, respectively. The maps are presented as a function of the fluid-entrance superficial velocities in the main pipe of the test section.

Experimental Results

Symmetric tee flow dividing system

Figure 4 shows the experimentally determined flow regime structure for the symmetric tee at the four observation points along the system. In all of the flow regime analyses of this article, the maps are presented as functions of the fluid-entrance superficial velocities in the main pipe of the system. The comparisons are made between the flow regime structure at each location and the fully developed straight pipe results as shown by dotted lines in Figure 4, as well as between theory and experiment for all of the flow dividing configurations.

Location L_1 (37 Pipe Diameters Upstream of the Junction). Difference between the dividing and straight pipe systems are apparent at low gas flow rates, Figure 4a. The stratified smooth section remains approximately the same; however, the stratified wavy section grows due to the acceleration of the fluid when it enters the tee. This acceleration causes the elongation gas bubbles to agglomerate and form a continuous stratified phase above an agitated water surface.

Location L_2 (14 Pipe Diameters Upstream of the Junction). The stratified smooth section is reduced in size due to the action of the fluid impinging on the far wall of the tee junction, Figure 4b. The reactive force of the wall on the fluid sends a continuous train of small amplitude waves upstream. Furthermore, the stratified wavy section increases in size due to the bubble agglomeration described above, and this effect becomes more pronounced closer to the junction.

Location L_3 (Two Pipe Diameters Upstream of the Junction). The stratified smooth section has been reduced in size due to the eddy motion caused by boundary layer separation in the region where the fluid turns, Figure 4c. At low gas flow rates there is a large growth of the stratified wavy section due to the halving of the flow rates when the fluids enter the two branches of the tee (and this causes a collapse of the plugs at the junction site). However, since the liquid requires time to change its velocity profile, low Reynolds number plugs may exist just down-stream of the junction. Furthermore, the liquid has the ability to climb up the far inner walls of the junction. If the liquid flow rate is sufficiently large, the water may carry over the top of the inner tube and bridge with the fluid on the opposite side forming an unstable plug.

The formation of the periodic annular churn and the periodic annular flow regimes correspond to the high energy associated with the slug flow in the main tube. The water slug, moving at a much greater speed than the rest of the liquid must dissipate its forward momentum when it enters the junction. It is done by wrapping itself around the inner wall of the tube. The water particles then move in a helical trajectory along the junction branch. The gas phase with a much lower momentum is able to slip "through" the swirling liquid annulus. The periodic annular churn regime is the limiting case of the periodic annular flow where the liquid annulus is unstable and collapses immediately on formation, trapping the gas as a bubbly core creating a churn-type pattern. In both of these regimes, the flow structure oscillates between an annular and a stratified wavy appearance with the same period of the slug in the main tube.

Location L_4 (25 Pipe Diameters Downstream and on Either Side of the Junction). It is obvious from the flow regime map for location L_4 that the flow is overdeveloped at this point, Figure 4d. The stratified smooth section has grown in size due to the dissipation of the small amplitude eddy waves created upstream at the junction. However, the large liquid surface disturbances created by the collapse of plugs at and near the junction location has prevented the stratified smooth transition boundary from recovering to its fully developed position.

At low gas flow rates, the stratified wavy to intermittent boundary has moved significantly due to the collapse of the unstable plugs that exist at the junction site. However, at high gas flow rates this boundary remains unchanged because the high energy slugs have sufficient momentum to sustain a considerable distance down the branch after the flow division. All of the intermittent flows at location L_4 may be described as slug because of the agitation caused in the fluid by the junction.

Several experimentally observed results of void fraction and pressure drop for various fluid superficial velocities (and hence flow regimes) are shown in Figures 5 and 6, respectively, for the symmetric tee. Here, the junction location is indicated by an arrow in the upper portion of the graph, and the dotted lines indicate a fully developed straight pipe flow result. The lines connecting the data points are not an interpolation of the experimental results, rather they are included to distinguish one data set from another. In Figure 6 and in all of the following pressure curves, the absolute value of pressure with respect to the first pressure tap is shown, hence (0,0) is a data point.

The behavior displayed in these figures will be discussed in this section, and different flow dividing structures will be compared in the next section. In the following discussion references to flow regime indicate the structure well upstream of the junction unless otherwise specified.

For the low gas flow rate stratified flows (curves 1, 2 and 6 in Figure 5), there is an increase in void fraction as the fluids approach the junction. After the junction, the void fraction is almost constant. As observed before, for these low gas flow rates, variation in the gas flow rate has no effect on the void fraction of pressure drop. The increase in void fraction along

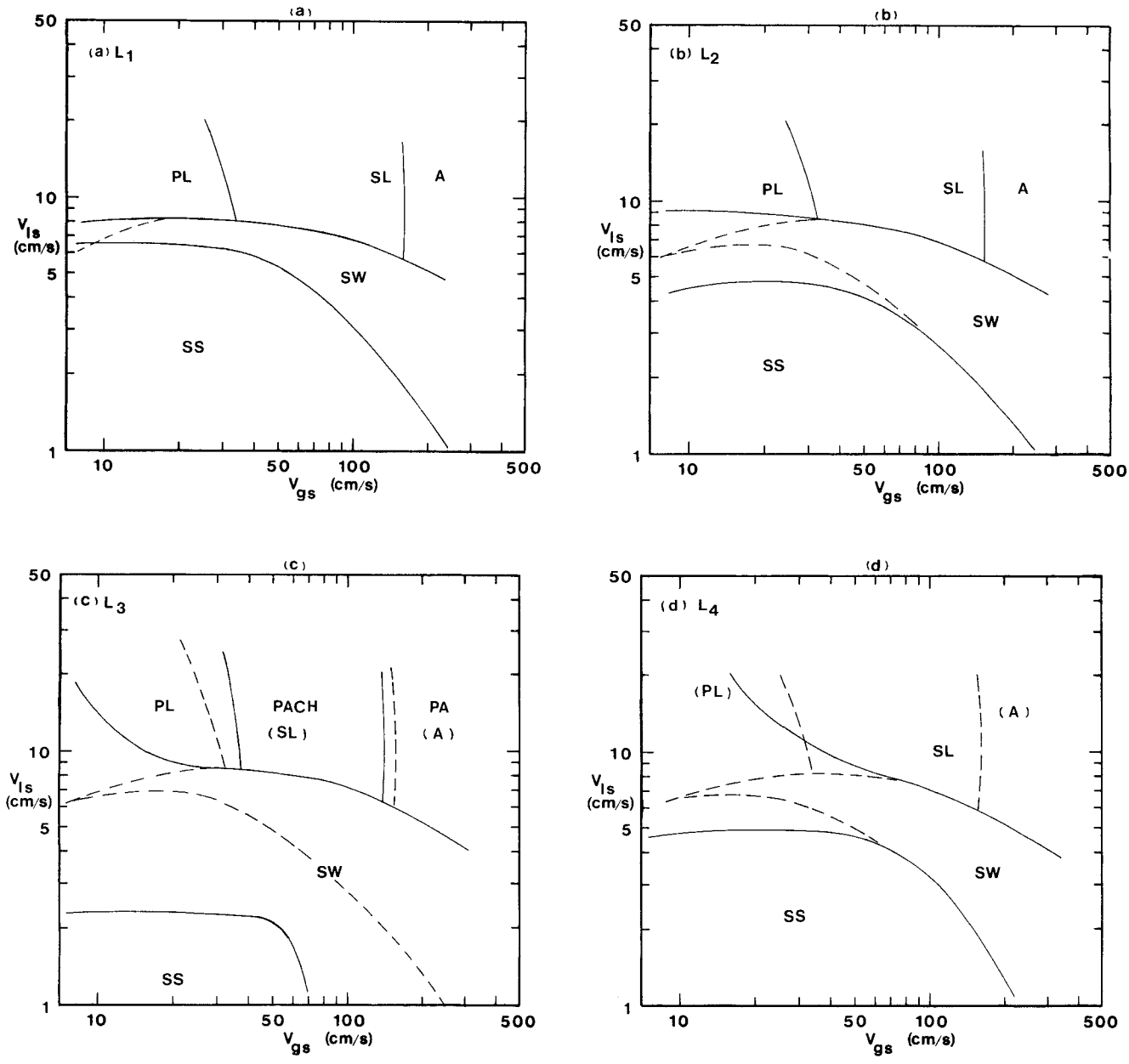

Figure 4. Experimentally observed flow regime maps for dividing tee system ($\theta = 90°$) for various locations.

a. 37 pipe diameters upstream of the junction L_1; b. 14 pipe diameters upstream of the junction L_2; c. two-pipe diameters upstream of the junction L_3; d. 25 pipe diameters downstream of the junction L_4.
- - - Straight pipe; —, tee pipe; J, tee junction.

the pipe upstream of the junction may be likened to an exit effect (due to the halving of the flow rates at the junction). This increase in voidage creates a corresponding increase in pressure drop due to the gravitational contribution.

For the stratified wavy flow (curve 3 in Figure 5), there is an overall increase in voidage across the junction due to the halving of flow rates. However, before the junction, there is a decrease in void. This is most probably due to an alteration in the gas velocity profile near the junction that allows the liquid level to rise.

Two instances of plug flow are shown in Figure 5 each with $u_{gs} = 10.6$ cm/s and one with $u_{ls} = 8.9$ cm/s, the other with $u_{ls} = 16.1$ cm/s. In the former case (curve 4 in Figure 5) the plug flow regime "collapses" into a stratified wavy structure, causing a significant increase in voidage before the junction. However, after the junction, there are no flow regime alterations (other than dissipation of the surface waves) and the void fraction remains constant.

For the later case of $u_{ls} = 16.1$ cm/s (curve 5 in Figure 5), the flow regime change occurs after the junction accounting, in part, for the large increase in void fraction observed there. Near, but just downstream of the junction, the void fraction is larger than "far" downstream of the junction because of the combined effect of fluid deceleration and the halving of the volume flow rates.

When the two fluids enter the junction they must decelerate

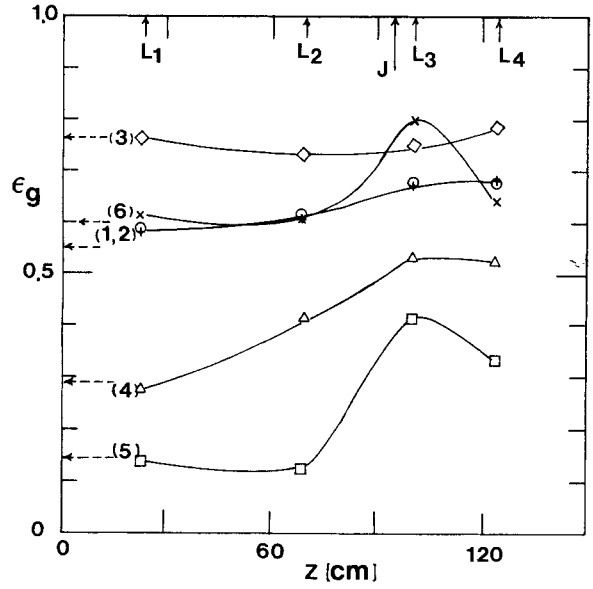

Figure 5. Experimentally observed axial void fraction behavior in a symmetric tee.

1. V_{ls} = 3.7 cm/s, V_{gs} = 10.6 cm/s (o o o)
2. V_{ls} = 3.7 cm/s, V_{gs} = 21.26 cm/s (+ + +)
3. V_{ls} = 3.7 cm/s, V_{gs} = 212.0 cm/s (◇ ◇ ◇)
4. V_{ls} = 8.9 cm/s, V_{gs} = 10.6 cm/s (△ △ △)
5. V_{ls} = 16.1 cm/s, V_{gs} = 10.6 cm/s (□ □ □)
6. V_{ls} = 16.1 cm/s, V_{gs} = 159.2 cm/s (XXX)

← - -, fully developed straight pipe; —, tee pipe

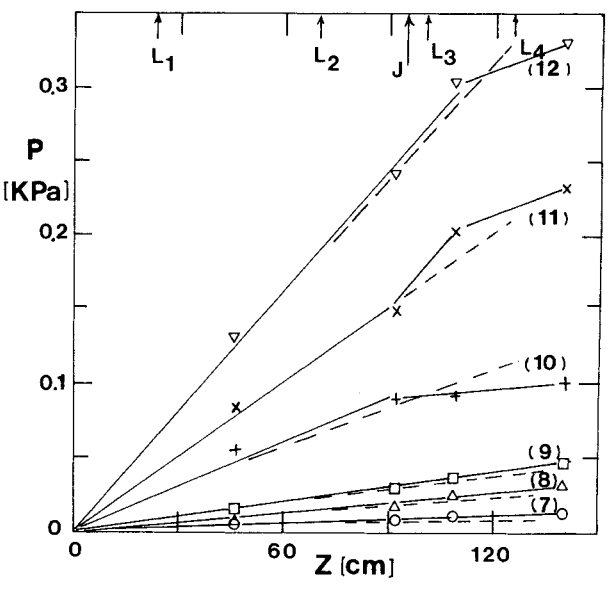

Figure 6. Experimental observed axial pressure behavior in a symmetric tee.

7. V_{ls} = 3.7 cm/s, V_{gs} = 10.6 cm/s (o o o)
8. V_{ls} = 8.9 cm/s, V_{gs} = 10.6 cm/s (△ △ △)
9. V_{ls} = 16.1 cm/s, V_{gs} = 10.6 cm/s (□ □ □)
10. V_{ls} = 16.1 cm/s, V_{gs} = 53.1 cm/s (+ + +)
11. V_{ls} = 16.1 cm/s, V_{gs} = 159.2 cm/s (XXX)
12. V_{ls} = 16.1 cm/s, V_{gs} = 265.0 cm/s (▽ ▽ ▽)

- - -, fully developed straight pipe; —, tee pipe

and come to their new velocities. The low-density gas phase decelerates quickly while the liquid moves through the junction with a velocity, near which it possessed just upstream of the flow division. This causes a large increase in voidage near the junction site. The above explanation for the flow behavior near the junction is verified numerically. It should be noted that there is no observable pressure recovery at the junction for the above mentioned flows (curves 8 and 9), and this effect is eliminated through the turbulent and gravitational losses.

One case of slug flow is shown in Figure 5 (curve 6). Before the junction, there is no effect on void fraction. This corresponds to the limiting case where information (specifically about the flow division) is transported only in the direction of momentum flow, and hence, the fluids do not "see" the junction until they arrive at the flow dividing site. A substantial increase followed by a decrease in void occurs along the system after the junction. The reasons for this behavior, namely flow division and deceleration, are discussed above.

Axial pressure distribution is shown for two cases of slug flow (curves 10 and 11 in Figure 6) and one case of wavy annular flow (curve 12 in Figure 6). Before the junction, the pressure drop is linear. At the junction site there is a significant change in pressure, the pressure drop across the junction increasing with increasing gas flow rate. Note that for none of the conditions shown here is there any pressure recovery at the junction. Presumably this is due to the irreversible losses caused by the tee in the fluids.

Comparison of experiment with theory for various flow dividing junctions

Figure 7 presents a comparison of the experimentally observed and theoretically predicted flow regime transition boundaries (Appendix I) in different symmetric tee and Wyes for each observation point along the test section. The flow regime boundaries for a straight pipe are included for reference.

Location L_1. Both the stratified smooth and stratified wavy boundaries move up at low gas flow rates, Figure 7a. Minor differences between regime structures may be considered due to experimental error.

Location L_2. A result similar to that above is observed at location L_2, except that the stratified smooth to stratified wavy transition for the symmetric tee occurs sooner than that for the straight pipe, Figure 7b. This early transition is due to the wave feedback mechanism described above and does not occur with Wye sections because of their construction. For both locations L_1 and L_2, the plug to slug boundaries agree with the straight pipe flow regime map.

Comparison of the theory with experiment for locations L_1 and L_2 indicates that in general the assumption that the flow structure does not change until it approaches very close to the junction is quite reasonable. The major exceptions to the above being the reduction in size of the stratified smooth regime due to the wave feedback mechanism and the enlargement of the stratified wavy regime due to the elongated bubble agglomeration. Both of these exceptions have the common characteristics of being low momentum flows.

Location L_3. For the stratified smooth to stratified wavy transition, agreement between theory and experiment is quite good, Figure 7c. The experimentally observed transitions occur at nearly the same locations as the theoretical predictions and show similar trends. At low gas flow rates, the shifting of the stratified wavy to intermittent transition boundary increases with decreasing junction angle and generally depends on the

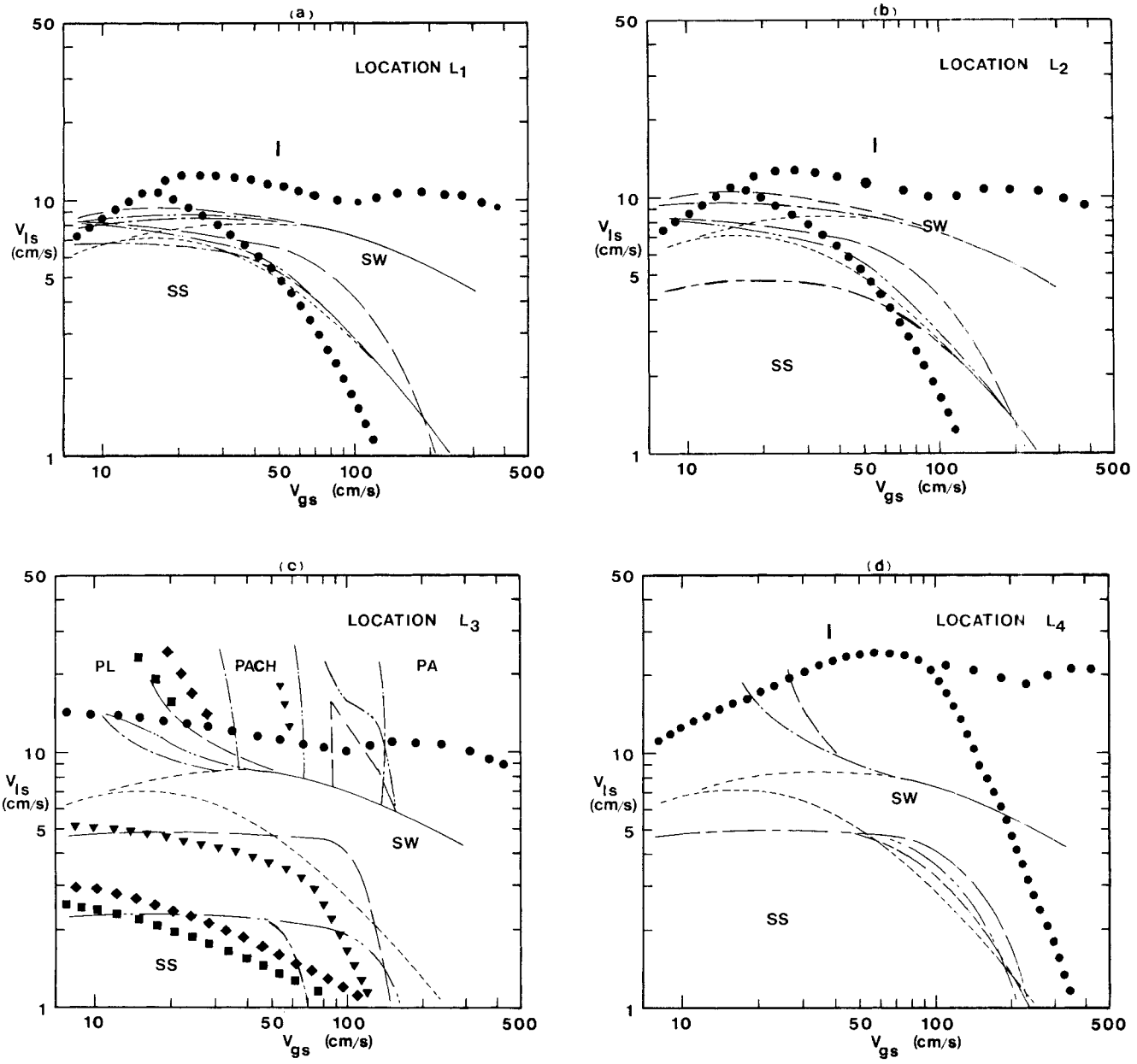

Figure 7. Experimentally observed flow regime vs. theory for various angles.

a. At location L_1 (37 pipe diameters upstream of the junction);
b. at location L_2 (14 pipe diameters upstream of the junction);
c. at location L_3 (two pipe diameters upstream of the junction);
d. at location L_4 (25 pipe diameters downstream of the junction).
Experiments: ——, all angles, - - -, 90°; -· -·-, 60° – –, 30°
Theory: ● ● ●, all angles; ■ ■ ■, 90°; ◆ ◆ ◆, 60°; ▼ ▼ ▼, 30°
Experimental results for straight pipe, - - - - - - -.

ability of the junction to form the liquid bridge that artificially creates an intermittent flow. While the theory predicts the general position of these transition boundaries well, it does not account for the formation of the unstable plugs and hence predicts no junction angle dependence for this transition.

Similar reasoning as above explains the shrinkage of the periodic annular flow regime, which is the ability of the large-angle Wyes to enhance the helical motion of the fluid particles since more of the fluid's forward momentum must be lost with increasing Wye angle. Theory agrees with the observed trend although it predicts that the flow regime transition should occur somewhat earlier than is observed. This discrepancy is most likely due to the fact that the theory has not accounted for the deceleration of the fluid as it approaches the junction and thus assumes much higher upstream slug speeds than are actually present.

Location L_4. The location of the stratified smooth to stratified wavy boundary for each type of Wye agrees with each other quite well; however, the flow is clearly overdeveloped. The slight shift that occurs in this boundary with changing

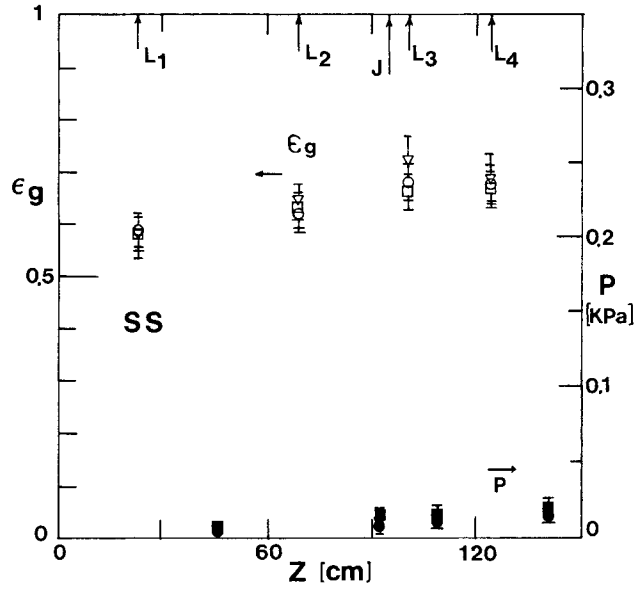

Figure 8. Experimentally observed two-phase behavior in various flow dividing junctions for a stratified flow.

V_{ls} = 3.7 cm/s; V_{gs} = 10.6 cm/s; o o ● ●, 90°; □ □ ■ ■, 60°; ▽ ▽ ▼ ▼, 30°
Theory: —, 90°; - - -, 60°; —·—, 30°

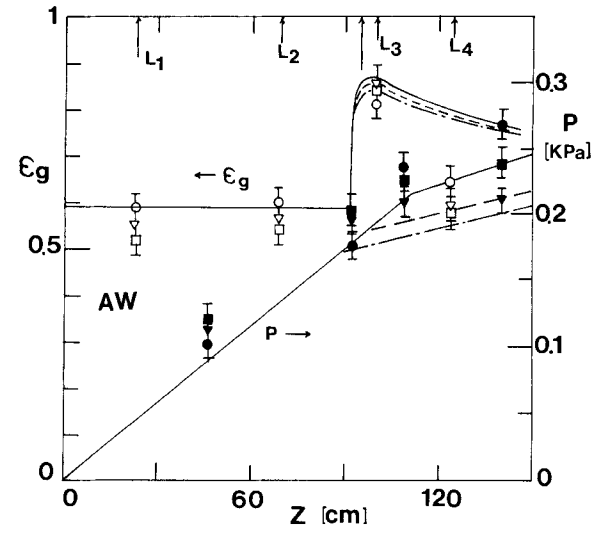

Figure 10. Observed and predicted two-phase behavior in various flow dividing junctions for a wavy annular flow.

V_{ls} = 16.1 cm/s; V_{gs} = 212.0 cm/s; o o ● ●, 90° □ □ ■ ■, 60°; ▽ ▽ ▼ ▼, 30°
Theory: —, 90°; - - -, 60°; —·— 30°

junction angle indicates the amplitude of the waves created at the junction. The tee junction creates the larger amplitude waves which, in turn, require greater distance to dissipate. As noted earlier, there is no change in the position of the stratified to intermittent boundary for high momentum flows.

Figures 8 and 9 depict the time averaged two-phase behavior of a stratified and a plug flow, respectively. As can be seen from these figures, there is no junction angle dependence, to within error, on the quantities measured. Thus, Figures 4, 5 and 6 apply to these flow structures.

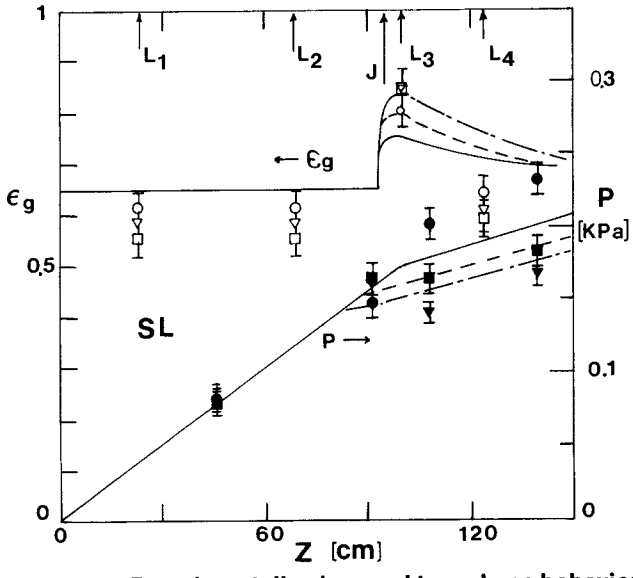

Figure 9. Experimentally observed two-phase behavior in various flow dividing junctions for a slug flow.

V_{ls} = 16.1 cm/s; V_{gs} = 159.2 cm/s; o o ● ●, 90°; □ □ ■ ■, 60°; ▽ ▽ ▼ ▼, 30°
Theory: —, 90°; - - -, 60°; —·—, 30°

With respect to the above mentioned low-momentum-type flows, no comparison with model predictions is possible as the numerical method used did not converge in these regions. Two possible reasons explain this problem:

1. *Numerical Method.* A simple upwind finite difference scheme was used here, although it may require a higher-order or more complicated scheme that lets information flow upstream.

2. *One-Dimensional Time-Average Model.* The restrictions, which this type of analysis imposes on the system, may be severe enough to remove the model far from reality.

For high-momentum flows (slug and wavy annular), a junction angle dependence is apparent as shown in Figure 10, in which the observed and predicted axial two-phase behavior are compared for different junction angles. In the model, the two constants Ω' and a are given for the values of 0.03 and 5.0, respectively. The large value of a indicates that the two-phase behavior changes drastically with decreasing junction angle as shown by the pressure distribution curves.

For all of the above mentioned curves, void fraction increases significantly at the junction, the size of the increase varying with flow rates. For high flow rates, the liquid speed upstream of the junction is large resulting in a large increase in void just downstream of the junction as discussed. The model predicts this general behavior quite well. To within error, no void fraction dependence on junction angle can be distinguished from the experimental data.

The general behavior (both void and pressure) depicted in these figures shows that before and after the flow division the flows are almost independent of the junction angle. It is also noted that in general the void fraction prediction downstream of the junction is consistently higher than that observed. This behavior can be best explained by the fact that at these points

the flows are in "transient" regimes and have a much higher momentum than they would possess in the linear system. Thus, the constitutive laws developed previously may not apply.

The pressure losses that occur at the junction can be quite large for the wavy annular type flows. In the regions strong junction angle dependence is apparent with significantly larger pressure drops occurring in the tee junction. This greater pressure drop in the large angle junctions is principally due to the losses incurred by the fluid as it turns. Clearly the symmetric tee, which requires a 90° turning of the fluid, will induce greater pressure losses in the system.

The two-phase system is capable of far greater losses at the junction than the equivalent single-phase system (by approximately one order of magnitude). This is due to the combined effects of periodically large liquid velocities, and change in void fraction and flow regime at the junction site. The inability of the model to consistently predict maximum pressure drop may be due to the lack of a flow regime energy loss term in describing the equations (a term depicting the energy lost in forming a new flow regime). The structure of such a term cannot be extrapolated directly from single-phase studies as there is no single-phase-equivalent. To determine the form of this loss factor, a much greater number of experiments need to be performed.

While, for the data presented here, pressure recovery does not occur in the tee, pressure recovery may occur in the smaller angle junctions. As is expected, greater pressure recovery is possible with decreasing junction angle. The model presented here, however, never predicts pressure recovery regardless of the junction configuration. This inconsistency arises from the Romie-type analysis, which always predicts a pressure loss at the flow division.

Conclusions

Experimental and theoretical investigations have been conducted to study the time-averaged void fraction, pressure drop and flow regime transition behavior of horizontal air-water two-phase flow in dividing horizontal tubes. Following concluding remarks are obtained:

- Two-phase behavior (flow regime, void fraction, and pressure drop) is strongly affected by the presence of a flow division in the system. These effects extend far upstream of the junction for low-momentum flows and far downstream for high-momentum flows.
- A method for predicting time-average pressure drop and void fraction in a two-phase flow, based on a two-fluid separated-flow model, has been proposed. The results and physical considerations show the method's validity.
- Using a two-fluid quasiseparated flow model, the axial time-averaged void fraction and pressure behavior was predicted. Numerical and experimental results show that a large increase occurs in void just downstream of the junction owing to the halving of the fluid volume rates and the liquid deceleration. In general, across the junction, there is an increase in voidage because of the flow division. Furthermore, the presence of junctions may produce either pressure recovery or significant pressure loss at the flow-dividing site with pressure loss always occurring for the symmetric tee.
- In general, the transition to stratified wavy flows occurs in a flow-dividing junction much earlier than in the straight pipe case. The exception being for the small-angled junctions where at high gas flow rates the shearing mechanism for wave generation dominates. The larger junction angles enhance this transition as expected, because the turning of the fluid is more severe.
- The transition to intermittent flow in the flow-dividing case may quite differ from that of the straight pipe system due to the removal of surface tension effects. However, the model accounts for no effect on this transition due to junction angle.
- For transition to annular-type flows, theoretical results show that formation of the swirling-type annular flow supersedes the formation of annular flow in the upstream linear section of the system. As expected, the formation of the swirling annular flow occurs earlier for the large-angle junctions. This transition may occur earlier for smaller-size pipes, simply because a lower slug velocity is required to overcome the gravitational acceleration.

Acknowledgment

The authors express their thanks to R. Girard, M. Shoukri, and S. T. Revankar for valuable discussions and comments. This work is supported by the Ministry of Universities and Colleges, the Ontario Government, Canada under, BILD grant and the Natural Sciences and Engineering Research Council of Canada.

Notation

A = fluid cross-sectional area, m^2
D = pipe diameter, m
D_j = hydraulic diameter for fluid j, m
f = friction factor
g = acceleration due to gravity, m^2/s
h = fluid level, m
k = separation constant
P = pressure, Pa
Q = flow rate, m^3/s
R = pipe radius, m
Re = Reynolds number
S = perimeter of pipe wetted by fluid, m
u = fluid velocity, m/s
V = volume, m^3
v = fluid velocity, m/s
W = mass flux
X = Blasius exponent
(X,Y) = cartesian coordinates describing plane normal to the axis of the tube
(x,y) = nondimensional cartesian coordinates describing plane normal to the axis of the tube
z = axial distance along the tube

Greek letters

ϵ = constant of integration
ϵ_g = void fraction (A_g/A)
θ = junction angle
λ = ratio of difference to summation of fluid viscosities
μ = viscosity, Pa·s
ρ = density, kg/m^3
σ = surface tension, Pa·m
τ = shear stress, N/m^2
Ψ = equilibrium shear stress distribution
Ω = general single-phase loss coefficient
$\Omega(\theta)$ = two-phase turning loss term
$\Omega'(\theta)$ = two-phase turning-momentum-exchange term

Subscripts

d = deviation
g = gas phase

gs = superficial gas
h = height
i = interface
j = signifies fluid j
ℓ = liquid phase
ls = superficial liquid
m = node value
s = slug
$\perp$ = perpendicular
$\parallel$ = parallel
o = constant
1 = upstream of flow perturbation or fluid 1
2 = downstream of flow perturbation or fluid 2
2Φ = mixed two-phase quantity

Superscripts

$*$ = reduced quantity
$'$ = perturbed quantity
n = iteration value

Abbreviations

A = annular
AW = annular wavy
ll = liquid phase and gas-phase laminar
tt = liquid-phase and gas-phase turbulent
lt = liquid-phase laminar and gas-phase turbulent
tl = liquid-phase turbulent and gas-phase laminar
PA = periodic annular
$PACH$ = periodic annular churn
PL = plug
SL = slug
SS = stratified smooth
SW = stratified wavy

Literature Cited

Azzopardi, B. J., and P. B. Whalley, "The Effects of Flow Patterns on Two-Phase Flow in a Tee-Junction," *Int. J. Multiphase Flow*, **8**, 491 (1982).

Ballyk, J. D., M. Shoukri, and A. M. C. Chan, "Steam-Water Annular Flow in a Horizontal Dividing T-Junction," *Int. J. Multiphase Flow*, **14**, 265 (1988).

Chang, J. S., R. Girard, R. Raman, and F. B. P. Tran, "Measurement of Void Fraction by Ring-Type Capacitance Transducers in Mass Flow Measurements," T. R. Hedrick and R. M. Reimer, eds., ASME Press, New York, **FED-17**, 93 (1984).

Chang, J. A., Y. Ichikawa, and G. A. Irons, "Flow Regime Characterization and Liquid Film Thickness Measurement in Horizontal Gas-Liquid Two-Phase Flow by an Ultrasonic Method," *Measurements in Two-Phase Flow*, T. R. Heidrick, ed., ASME, 7 (1982).

Fouda, A. E., and E. Rhodes, "Two-Phase Annular Flow Stream Division in a Simple Tee," *Trans. Int. Chem. Engrs.*, **52**, 354 (1974).

Fouda, A. E., and E. Rhodes, "Two-Phase Annular Flow Stream Division," *Trans. Int. Chem. Engrs.*, **50**, 353 (1972).

Henry, J. A. R., "Dividing Annular Flow in a Horizontal Tee," *Int. J. Multiphase Flow*, **7**, 343 (1981).

Honan, T. J., and R. T. Lahey, "The Measurement of Phase Separation in Wyes and Tees," *Nuc. Eng. Design*, **64**, 93 (1981).

Lightstone, L., and J. S. Chang, "Flow Regime Observation in Horizontal Two-Phase Dividing Flow in Tees and Wyes," *Proc. Cdn. Chem. Eng. Conf.*, **1**, 281 (1983).

Lottes, P. A., "Expansion Losses in Two-Phase Flow," *Nuc. Sci. Eng.*, **9**, 29 (1961).

Mandhane, J. M., G. A. Gregory, and K. Aziz, "Flow Pattern Map for Gas-Liquid Flow in Horizontal Pipes," *Int. J. Multiphase Flow*, **1**, 537 (1974).

Matikainen, L., G. A. Irons, E. C. Morala, and J. S. Chang, "Ultrasonic System for the Detection of Transient Liquid/Gas Interfaces Using the Pulse-Echo Technique," *Rev. Sci. Instrum.*, **57**, 1661 (1986).

McCreery, G. E., "A Correlation for Phase Separation in a Tee," *Multiphase Symp.*, Miami (1983).

McNown, J. S., "Mechanics of Manifold Flow," *Trans. ASCE*, **119**, 1103 (1954).

Modi, P. N., P. D. Ariel, and M. M. Dondekar, "Conformal Mapping for Channel Junction Flow," *Proc. ASCE*, **107**, 1713 (1981).

Osamusali, S. I., and J. S. Chang, "REGIME-4 Code for Prediction of Flow Regime Transition in a Horizontal Pipe, Annulus and Bundle Flow under Gas-Liquid Two-Phase Flow," *Proc. Can. Nucl. Soc.*, Meeting, J. D. Summerville, ed., 125 (1987).

Pollard, A., "Computer Modeling of Flow in Tee-Junctions," *Phys. Chem. Hydrody.*, **2**, 203 (1981).

Pollard, A., and D. B. Spalding, "The Prediction the Three-Dimensional Turbulent Flow Field in a Flow-Splitting Tee-Junction," *Comput. Meth. App. Mech. Eng.*, **13**, 294 (1978).

Pollard, A., and D. B. Spalding, "On the Three-Dimensional Laminar Flow in a Tee-Junction," *J. Heat Mass Transfer*, **23**, 1605 (1980).

Reimann, J., and W. Seeger, "Two-Phase Flow in a T-Junction with a Horizonal Inlet: Part II. Pressure Differences," *Int. J. Multiphase Flow*, **12**, 587 (1986).

Schutt, H. C., *Trans. ASME*, **HYD 51**, 83 (1929).

Seeger, W., J. Reimann, and V. Miller, "Two-Phase Flow in a T-Junction with a Horizontal Inlet: I. Phase Separation," *Int. J. Multiphase Flow*, **12**, 575 (1986).

Taitel, Y., and A. E. Dukler, "A Model for Predicting Flow Regime Transitions in Horizonal and Near Horizontal Gas-Liquid Flow," *AIChE J.*, **22**, 47 (1976).

Tsuyama, M., and M. Taga, "On the Flow of the Air-Water Mixture in the Branch Pipe," *Bull. JSME*, **2**, 151 (1959).

Appendix 1: Predictions of Flow Regime Transitions Downstream of the Junction

The approach applied here is to assume that the flow regime structure does not change until the fluid arrives at the junction and that the flow structure downstream of the junction depends strongly on the upstream structure. In other words, the flow regimes will depend on upstream velocities, rather than local velocities.

Clearly, this model will not apply to some distance downstream of the junction but it will predict the flow structure at the junction site that may be considered as a type of extreme. In this model, the methods of Taitel and Dukler (1965) and Osamusali and Chang (1987) are used to analyze flow regime transitions, where a simple one-dimensional momentum balance on each phase is assumed, and following transition creation is used in addition to Taitel and Dukler's and Osamusali and Chang's models.

Transition to stratified wavy flow

When a fluid flows around an object, for example, a cylinder, eddying motion may be induced in the liquid through boundary layer separation. The criterion for the onset of separation is usually given in terms of a critical Reynolds number:

$$(Re)_{\text{crit}} = \frac{\rho u L}{\mu} \tag{A1}$$

Here the viscosity and speed are the characteristics of the fluid, and the length is a characteristic of the object over which the fluid passes.

For the situation of fluid turning at a junction of angle θ, the characteristic length may be conveniently defined as $R\sin\theta$. Regime transition would occur when this turning Reynolds number has a value of several hundred or

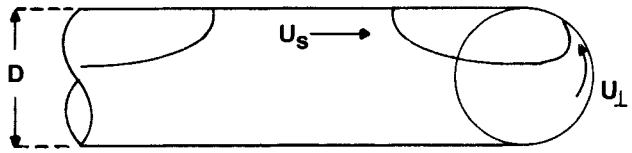

Figure A1. Swirling annular flow formation at junction site.

$$u_\ell = \frac{\mu_\ell (Re)_{\text{crit}}}{R\rho_\ell \sin\theta} \tag{A2}$$

Based on present experimental results, the value of Re_{crit} used in this study is 350. This Reynolds number does not represent the conditions at which boundary layer separation occurs, but rather indicates when the eddying motion induced by boundary layer separation becomes significant.

Transition from intermittent to periodic annular flow

When considering this flow regime transition, it is assumed that the upstream flow structure is intermittent. The slug travels toward the junction as shown in Figure A1 with a speed u_s relative to the pipe wall. u_s may be determined by material balance as:

$$u_s = u_{\ell s} + u_{gs} \tag{A3}$$

It is well known that a turning fluid develops secondary spiral-type flows. Once the liquid enters the junction, it will tend to wrap itself around the inner wall. The fluid in the junction may be said to possess two components of velocity: one representing a swirling type of flow $u_\perp$ and the other, $u_\parallel$, representing the flow parallel to the branch axis. The magnitude of the fluid velocity in the junction is the square root of the sum of the squares of the two components.

For the situation in Figure A1, the junction angle is 90°. Naturally, the dependence of $u_\perp$ on the junction angle is expected. The following form appears to be plausible:

$$u_\perp(\theta) = \frac{u_\perp}{\sin\theta} \tag{A4}$$

The formulation fits the extreme condition, where $\theta = 0$, that is, an infinite velocity is required to produce a secondary swirling flow.

As the fluid enters the junction, the condition for the fluid to wrap itself around the wall is that the swirling component of the velocity be sufficient to provide the fluid particles with the centripetal acceleration necessary to overcome gravity.

$$u_\perp(\theta) = \frac{1}{\sin\theta}\sqrt{Rg} \tag{A5}$$

The speed of the slug along the branch axis before and after the junction is related to continuity. For the simple symmetric flow-dividing junctions under consideration in this study $u_s = 2u_\parallel$. Furthermore, it is assumed that the fluid in the slug and in the swirling annulus is equally distributed throughout the pipe with respect to the pipe axis so that gravitational energy terms may be discounted. Applying a Bernoulli type analysis at the junction

$$u_s^2 = u_\perp^2(\theta) + u_\parallel^2 \tag{A6}$$

or

$$u_{\ell s} + u_{gs} = \frac{1}{\sin\theta}\sqrt{\frac{4}{3}Rg} \tag{A7}$$

Note that unlike the previous transition criteria, this transition does not depend on a stratified liquid level. This is because the preexistence of slug rather than stratified flow has been assumed.

The theoretical effect of the flow-dividing junction on the regime structure just downstream of the junction is shown in Figure 7d for junction angles as a function of fluid entrance superficial velocities in the main pipe. In general, the transition to stratified wavy flow occurs in a flow dividing junction much earlier than in the linear case. The exception being for the small angled junction where at high gas flow rates the shearing mechanism for wave generation dominates. The larger junction angles enhance this transition, as expected, because turning of the fluid is more severe. Similarly, the enhancement of this transition occurs for increasing pipe diameters.

The transition to intermittent flow in the flow-dividing case quite differs from that of the straight pipe system due to the removal of surface tension effects. However, the model accounts for no effect on this transition due to junction angle and furthermore indicates a negligible tube diameter effect.

For transition to annular-type flows, theoretical results show that formation of the swirling-type annular flow supersedes the formation of annular flow in the upstream linear section of the system. As expected, the formation of the swirling annular flow occurs earlier for the large-angle junctions. This transition also occurs earlier for the smaller-size pipes, simply because a lower slug velocity is required to overcome the gravitational acceleration.

Manuscript received Feb. 14, 1990, and revision received Nov. 26, 1990.